Title

Extracellular enzyme kinetics and thermodynamics along a climate gradient in southern California

Authors

Baker, Nameer R
Allison, Steven D

Publication Date

2017-11-01

DOI

10.1016/j.soilbio.2017.07.005

Peer reviewed

Highlights

- Extracellular enzyme activity (V_{max}), substrate affinity (K_m), and the temperature sensitivity of V_{max} and K_m were established along a Mediterranean climate gradient in southern California.
- Fungal biomass, potential proteolytic activity, and substrate availability best explained variation in enzyme V_{max} and K_m along the gradient.
- V_{max} and K_m displayed positive temperature sensitivity along the gradient, and V_{max} temperature sensitivity exhibited a negative relationship with site mean annual temperature during the wet season.

Title

Extracellular enzyme kinetics and thermodynamics along a climate gradient in southern California

Authors

Nameer R. Baker[a,1] and Steven D. Allison[a,b]

[a]Department of Ecology and Evolutionary Biology, University of California, Irvine, CA 92697, USA

[b]Department of Earth System Science, University of California, Irvine, CA 92697, USA

[1]Present address: Department of Environmental Science, Policy, and Management, University of California, Berkeley, CA 94709, USA

Correspondence:

Nameer R. Baker

2151 Berkeley Way, Berkeley, CA 94709, USA

nameer@berkeley.edu

Keywords

Climate gradient, microbial decomposers, extracellular enzymes, substrate affinity, temperature sensitivity

Abstract

Microbial decomposers produce extracellular enzymes to degrade complex plant polymers, making plant C available for metabolism and eventual respiration back to the atmosphere as CO_2. Knowledge of how extracellular enzyme kinetics and microbial activity vary with climate is therefore valuable for predicting how future carbon cycling may be affected by climate change, but studies investigating such dynamics in more xeric ecosystems are underrepresented in the literature. We investigated how microbial biomass, litter chemistry, and extracellular enzymes (V_{max} and K_m) and their temperature sensitivities varied along a Mediterranean climate gradient in southern California. Total microbial biomass did not vary among sites along the gradient in either the dry or the wet season. In contrast, extracellular enzyme V_{max} and K_m varied as a function of fungal biomass and substrate availability. We also found that V_{max} and K_m of most enzymes were more sensitive to temperature in colder sites than in warmer sites, though this relationship was seasonal for V_{max}. Observed enzyme V_{max} and K_m were indicative of extracellular enzyme accumulation in the drier sites along the gradient, which may contribute to the large pulses of respiration that follow rewetting events in these xeric systems. Variation in enzyme characteristics along the gradient indicate that as these systems become more arid in the future, enzyme dynamics will shift from smaller, potentially more active pools to larger, potentially less active enzyme pools that accumulate over dry periods. In addition, rates of enzymatic decomposition will likely be most sensitive to rising temperatures in the coldest sites along our gradient.

1. Introduction

Many microbes secrete extracellular enzymes (EE) capable of degrading complex biological polymers into bio-available compounds that fuel metabolism and respiration (Burns et al., 2013; Sinsabaugh et al., 1994). These processes account for a substantial fraction of ecosystem respiration from soils and litter (Raich and Schlesinger, 2002) and are affected by abiotic climate variables such as moisture and temperature that alter diffusion, reaction rates, and osmotic potential. In addition to these direct effects, climate indirectly shapes microbial communities by exerting strong control on the composition of plant communities (IPCC, 2014), thereby determining substrate availability for microbial decomposers (Saleska et al., 2002).

EE catalysis of complex organic substrate degradation is the rate-limiting step in returning C from plant detritus to the atmosphere (Sinsabaugh and Shah, 2011), though physical protection of C and diffusion constraints can supersede the importance of enzyme catalysis in mineral soils (Schimel and Schaeffer, 2012). These substrates vary, from highly accessible disaccharides and starches to more chemically complex compounds such as hemicellulose, cellulose, and lignin. In the last few decades, decomposition dynamics have been related to microbial activity and assays of EE kinetics in a host of studies (Allison et al., 2007; see also references in Burns et al., 2013 and Sinsabaugh et al., 2008), but investigations of how EE characteristics vary in xeric ecosystems is lacking. In a 2008 global meta-analysis of EE activity in soils, 10% or fewer of the sites were located in dryland ecosystems (Sinsabaugh et al., 2008), even though drylands make up ~40% of terrestrial ecosystems by land area (MEA, 2005).

This knowledge gap is significant because decomposition models validated in mesic ecosystems and built around temperature, moisture, and litter chemistry consistently underestimate rates of decomposition in more xeric drylands ecosystems, such as semiarid

Mediterranean grasslands and arid deserts (Whitford et al., 1981). As such, conclusions drawn from decomposition dynamics and EE kinetics observed in mesic ecosystems may not be applicable to more xeric ecosystems. This uncertainty complicates efforts to predict future carbon dynamics, especially given that xeric ecosystems are projected to become hotter and drier. This is especially true for the American Southwest, where models are remarkably consistent in predicting a shift to a more arid climate beginning in the early part of the 21st century (Seager et al., 2007) and where temperatures are projected to rise by 2.5-5.5° in the next fifty years if global emissions continue to increase (Garfin et al., 2014). Determining how enzyme kinetics vary with climate in such drylands ecosystems is therefore a necessary step in predicting how decomposition rates in these systems may be affected by future climate change.

EE kinetics can be described by the Michaelis-Menten model, whereby activity (V) of an individual enzyme is described as a saturating function of substrate (S) concentration:

$$V = V_{max}[S]/(K_m + [S])$$

where V_{max} is the enzyme's maximum reaction rate and K_m, the half-saturation constant, is the substrate concentration at which the reaction rate is one-half V_{max}. Given that enzyme concentrations *in situ* are controlled by feedbacks between microbial activity and substrate availability, conditions that are conducive to high EE V_{max} should therefore also be conducive to high K_m (Wallenstein et al., 2011). This is because high substrate availability makes enzymatic reactions proceed more quickly, resulting in more products that can be absorbed by microbial cells to fuel further enzyme biosynthesis. While we expect EE kinetic parameters to vary as a function of microbial activity (Sinsabaugh et al., 1994), thermodynamic theory predicts that V_{max} and K_m will also increase with increasing temperature (Davidson and Janssens, 2006), which has potential implications for future C-cycling. Increasing temperature can allow more reactants to

attain their activation energies, increasing V_{max}. At the same time, the stability of the substrate-enzyme complex may be reduced, causing decreased substrate affinity and higher observed K_m (Johns and Somero, 2004; Sørensen et al., 2015).

Increases in temperature should have reduced effect on the kinetic parameters of EEs from colder environs (Siddiqui and Cavicchioli, 2006), especially if enzymes are locally adapted (Belotte 2003). This is because cold-adapted organisms optimize enzyme efficacy at low temperatures by minimizing reaction activation energy, or E_a (Georlette et al., 2004; Lonhienne et al., 2000), and V_{max} temperature sensitivity increases as E_a increases according to the Arrhenius relationship (Davidson et al., 2006). Organisms optimized for higher temperatures have relaxed selection for minimizing E_a because their enzymes and substrates have greater kinetic energy. Given that changes in V_{max} and K_m are generally correlated (Sinsabaugh et al., 2014), it is reasonable to assume that K_m temperature sensitivity may exhibit similar patterns as those hypothesized for V_{max} based on thermodynamic theory. Evidence from natural systems is generally lacking in the literature, but several published studies seemingly contradict these expectations: Koch et al. (2007) found that EE temperature sensitivities increased at lower temperatures in alpine soils assayed across three seasons, and both they and Wallenstein et al. (2009) found that EE temperature sensitivity declined over the growing season in alpine and arctic tundra soils, respectively. However, this hypothesis has never been tested along a regional climate gradient, where microbial communities are unlikely to be dispersal limited with regards to the pool of regional taxa (Kivlin et al., 2011), and local climate variation is likely to be a strong filter.

The goal of this study is to use a climate gradient across xeric ecosystems of southern California to determine how microbial EEs might respond to long-term climate change. Along

111 this gradient, temperature and moisture co-vary, such that hotter, drier sites at low elevations
112 contrast with colder, wetter sites at higher elevations. As such, moving from higher to lower
113 elevations mimics the shift to more arid climates expected in the American Southwest. Litter
114 lignin content and the size of the litter pool also generally decrease when transitioning from
115 higher to lower elevations. We aimed to quantify the environmental drivers of enzyme kinetic
116 parameters along the climate gradient to advance knowledge of biogeochemical mechanisms in
117 xeric ecosystems. Based on the above theory, we formulated the following hypotheses:

118 **1.** Microbial biomass, EE V_{max}, and EE K_m will increase with increasing precipitation, as
119 moisture and substrate availability limit microbial activity which in turn limits EE
120 production.

121 **2.** V_{max} and K_m of enzymes from colder, wetter sites will be less temperature sensitive, and
122 enzymes assayed in the wet season will be less temperature sensitive than those assayed in
123 the dry season.

124 We tested these hypotheses by measuring microbial properties, litter substrates, and enzyme
125 kinetics along a climate gradient spanning 12.5 °C and 300 mm precipitation in southern
126 California.

127

128 **2. Materials and methods**

129 *2.1 Site description*

130 To test how EE kinetic parameters and thermodynamics varied with climate, we assayed
131 plant litter from five sites representing five biomes in southern California – Colorado desert (lat,
132 long: 33.652, -116.372), pinyon-juniper scrubland (33.605, -116.455), coastal grassland (33.737,
133 -117.695), pine-oak forest (33.808, -116.772), and subalpine forest (33.824, -116.755). All five

sites are located on granitic parent material and experience Mediterranean precipitation patterns (cool, wet winters; hot, dry summers). The desert is on a deposit of Carrizo stony sand, and is dominated by desert perennials and annuals. The scrubland is on an Omstott coarse sandy loam, and is dominated by pinyon pine, juniper, and desert perennials and annuals. The grassland is on a Myford sandy loam, and is dominated by annual grasses and forbs, particularly *Bromus* and *Avena* spp. The pine-oak forest is on a Pacifico-Preston families soil complex and is dominated by pines as well as evergreen and deciduous oak. The subalpine site is on a rocky outcrop of granite that lies among a Pacifico-Wapi families soil complex, and is dominated by lodgepole and limber pine. The gradient spans a range of ~12.5 °C in mean annual temperature (MAT), from 22.8±0.8 °C at the desert site to 10.3±1.8 °C at the subalpine site (**Table 1**). The desert site experienced the least mean annual precipitation in the form of rainfall over the five years prior to this study (100±24 mm), and the pine-oak forest (hereafter referred to as "pine-oak") site experienced the most (400±120 mm). Standing litter pools are largest in the grassland and pine-oak site, reduced in the subalpine site, significantly reduced in the scrubland site, and negligible in the desert site (personal observation). Air temperature, soil temperature, rainfall, and solar radiation data for all sites other than the subalpine site come from eddy covariance towers at each site.(Goulden et al., 2006). Two iButton temperature sensors (Maxim Integrated) were also installed at each site on January 18, 2015, to collect surface temperature at 90 minute intervals until the final sampling date on December 2, 2015.

2.2 Sampling

Local plant litter was collected from each of the five sites on June 7, and December 2, 2015. Along this gradient, these dates correspond to the beginning of the dry season and

157 increased litterfall throughout May and into June and the early-middle of the wet season in
158 December. As such, litter collected in June was recently deposited and had been exposed to
159 rising temperatures in the preceding months, whereas litter collected in December fell in late
160 spring or early summer and would have been subject to a cooling trend and increased
161 decomposition in the interim. Using gloves, 5 g litter was collected from the soil surface of each
162 site by lightly raking across the surface to collect loose material and using clippers to detach
163 senescent grass litter from root bundles if necessary. Litter replicates were collected from six 0.5
164 m^2 plots established within a 50 m^2 radius of one another at each site. Collected litter was stored
165 in coolers and transported to UC Irvine, where it was ground into fragments <0.5cm in length
166 and sub-sampled for EE assays and biomass of bacteria and fungi. The remaining litter was
167 weighed and oven-dried to determine moisture content.
168
169 *2.3 Litter chemistry*
170 Oven-dried litter was sent to Cumberland Valley Analytical Services for near-IR
171 spectroscopy, whereby reflectance spectra of near-infrared wavelengths of light are matched to a
172 verified database of spectra for plant materials with known chemical compositions previously
173 established by wet chemistry. This method has been shown to be more accurate and more
174 repeatable than wet chemistry analysis for a diverse range of crop and tree residues (Shepherd et
175 al., 2005). Relative amounts of the following organic compounds were determined as proportions
176 of total dried litter mass: lignin, cellulose (acid detergent fiber – lignin), hemicellulose (neutral
177 detergent fiber – acid detergent fiber), non-structural carbohydrates, structural carbohydrates
178 (non-fiber carbohydrates – non-structural carbohydrates), and crude protein. The non-structural
179 carbohydrate fraction consists of starches and sugars, whereas the structural carbohydrate

fraction includes plant cell components such as pectins, but also microbial cell wall components such as β-glucans and peptidoglycans (CVAS, *personal communication*).

2.4 Extracellular enzyme assays, kinetics, and thermodynamics

In assays of EEs from ecological systems, V_{max} and K_m are measured as apparent parameters, ${}^{app}V_{max}$ and ${}^{app}K_m$. ${}^{app}V_{max}$ does not represent the reaction rate of a single enzyme, but instead indicates the overall concentration of enzymes in a sample that degrade a particular class of substrates (Wallenstein et al., 2011). ${}^{app}K_m$ does not represent a single enzyme's substrate affinity, but instead reflects relative substrate availability because the fluorescently labeled substrates added during EE assays compete for enzyme active sites with naturally occurring substrates already present in environmental samples (Chróst, 1990). Thus, for a given substrate concentration, the observed reaction velocity will be lower than its actual in-assay value and its corresponding K_m will be higher, because some natural non-fluorescently labeled substrates will also be cleaved. For simplicity, ${}^{app}V_{max}$ and ${}^{app}K_m$ at 22 °C are presented as V_{max} and K_m throughout the text.

Litter was assayed for V_{max}, K_m, and the temperature sensitivities of V_{max} and K_m for seven hydrolytic enzyme classes using fluorescently labeled substrates based on German et al. (2012). The enzyme classes assayed were as follows: *α*-glucosidase (AG), acid phosphatase (AP), *β*-glucosidase (BG), *β*-xylosidase (BX), cellobiohydrolase (CBH), leucine-aminopeptidase (LAP), *N*-acetyl-*β*-D-glucosaminidase (NAG). 125µL of fluorometric substrate solution was combined with 125µL of litter homogenate in each microplate well. Substrate solutions, standard controls, and litter homogenate were made in 25 mM maleate buffer with pH 6.0. Litter was stored at -80 °C and homogenate was made using 0.4 g frozen litter in 150mL buffer. A

reference standard was used, and the quench coefficient was calculated by dividing the fluorescence of the reference standard in wells with litter homogenate by its fluorescence in wells with just buffer. Assays were incubated for 4h at 4, 10, 16, 22, 28, or 34°C. Each enzyme was assayed at a range of eight substrate concentrations for each temperature (**Table S1**), where the highest concentration was previously established to saturate enzymes in solution (German et al., 2011). Negative potential activities were considered to indicate that no enzyme was present, and were converted to zero values before further analyses.

EE kinetic parameters were calculated for each enzyme class and incubation temperature by fitting observed EE activity at each substrate concentration to the Michaelis-Menten equation. Non-linear regressions were performed in the R software environment 3.3.1 (R Development Core Team, 2016) using the nls function. Confidence intervals were determined for V_{max} and K_m values using the nlstools package. Fits of V_{max} with a 95% CI greater than twice the magnitude of V_{max} were discarded; because of greater variability in calculated fits of K_m, fits with a 95% CI greater than four times the magnitude of K_m were discarded.

Temperature sensitivities of EE kinetic parameters for each enzyme class were determined by linear regression of ln V_{max} or ln K_m against incubation temperature. Regressions were performed using the lm function in R. Regressions with $R^2 < 0.50$ were discarded. Slopes were converted to Q_{10} values as in Wallenstein et al. (2009) using the formula:

$$Q_{10} = \exp(\text{slope} \times 10)$$

2.4 Microbial biomass

Litter bacterial cell density was estimated by methods identical to those in Allison et al. (2013). In brief, ground litter was suspended in a phosphate-buffered, 1% glutaraldehyde

226 solution on the day of sample collection to "fix" bacterial cells for storage. Within two weeks,
227 0.1 M tetrasodium pyrophosphate was added to each sample, and samples were sonicated to
228 dislodge bacterial cells. These extracts were passed through 2.7 μm filters to remove particulate
229 matter before being stained with 1x SYBR-Green. Stained extracts were run on an Accuri C6
230 flow cytometer to determine cell counts from fluorescing bacterial cells that exceeded the 2000
231 limit on the FLH1 channel and appeared distinct from particulate noise when comparing the side-
232 and front-scatter of reflecting light.

233 The length of fungal hyphae in litter was measured by adapting methods used in Allison
234 et al. (2013). Ground litter was suspended in 0.395% (w/V) sodium hexametaphosphate and
235 vigorously stirred before being vacuum-filtered and stained with acid fuchsin. Two filters 17 mm
236 in diameter were made for each litter sample and affixed to a glass slide. Hyphal lengths were
237 measured with a Carl Zeiss photomicroscope at 100X magnification using Axioplan 2 Imaging
238 software. Hyphal lengths were measured in 89 x 67 μm viewing panes using 30 panes per slide
239 (15 per filter). Total hyphal length in all viewing panes for a single sample was converted to
240 estimates of hyphal length in meters per gram of dry litter using a modified procedure of Sylvia
241 (1992).

242 Bacterial cell density and fungal hyphal lengths were converted to bacterial and fungal
243 biomass (mg C g^{-1} dry litter) and combined to estimate total microbial biomass C using methods
244 identical to those in Alster et al. (2013). In brief, bacterial cells were assumed to be spherical
245 with a radius of 0.6μm and C density of 2.2 x 10^{-13} g um^{-3} (Bratbak, 1985), and fungal hyphae
246 were assumed to have a fresh density of 1.1g per cm^{-3} of hyphae, 33% dry mass, 40% C in dry
247 mass, and diameter of 5.2 μm (Paul and Clark, 1996). Bacterial cell counts from June 2015
248 samples could not be assayed because of technical issues with the flow cytometer; as such,

bacterial cell densities, fungal hyphal lengths, and EE V_{max} and K_m from litter collected in identical fashion on October 16, 2014 were used to determine seasonal variation of microbial biomass as well as any relationships between microbial biomass and EE parameters. These time points were deemed comparable because a concurrent study indicated that microbial decomposer activity is greatly reduced throughout the dry season in these sites.

2.5 Statistical methods

Effects of site and sampling date on microbial and fungal biomass were analyzed using mixed-model ANOVA with the identity of each plot as a random factor. Because litter moisture is known to be a strong control on decomposition processes in Mediterranean ecosystems, the model was run as an ANCOVA with litter moisture content as the covariate. ANCOVA was also used to determine if there was a relationship between total microbial biomass or fungal biomass and V_{max} or K_m across sites. Post hoc analyses of pairwise comparisons were done with Tukey contrasts using the lsmeans package in R.

Effects of site and sampling date on litter chemistry, V_{max}, K_m, V_{max} temperature sensitivity, and K_m temperature sensitivity of all EE classes were determined by MANCOVAs containing the relevant parameters for all EE classes with litter moisture content as a covariate, using the Wilks Lambda method to calculate the test statistic. Differences in EE profiles, climate, and litter chemistry between sites were determined by canonical discriminant analysis (CDA). Data for ANCOVAs and MANCOVAs were checked for normality visually using quartile-quartile plots of residuals and by the Shapiro-Wilk test, and non-normal data were natural log-transformed to improve normality when necessary. Microbial and fungal biomass met assumptions of normality after ln-transformation; ln V_{max} and ln K_m did not but passed visual

inspection. Litter chemistry fractions and temperature sensitivities of V_{max} and K_m did not meet assumptions of normality but were visually determined to be approximately normal when in base form, and as such were not transformed prior to statistical analyses.

Recent mean annual air temperature at the subalpine site was extrapolated from a linear regression ($R^2 > 0.8$) of elevation versus air temperature observed by the four eddy covariance towers and a Remote Area Weather Station (RAWS) located at the summit of Mt. San Jacinto (2626 m above sea level, 2.5 km from the subalpine site, and also on the windward side of the range). Recent rainfall, solar radiation, and daily temperature range at the subalpine site could not be extrapolated from the RAWS data, but the values observed at Mt. San Jacinto are presented for the subalpine site to provide context given the proximity and likely similarity between the two locations.

CDA indicated that most climate variables measured by the eddy covariance towers were positively correlated. As a result, air temperature was used for climate-related analyses because of our high confidence in extrapolated air temperature at the subalpine site. Linear regression was then used to determine if site air MAT explained a significant amount of the variation in V_{max} and K_m temperature sensitivities observed in either June or December 2015.

3. Results

3.1 Climate gradient

Recent climate observed by the four flux towers followed a similar trend for air MAT, soil MAT, soil moisture, rainfall, and mean daily ranges for air and soil temperature. The desert and pine-oak sites were at the two extremes for each variable, and the grassland and scrubland experienced similar, intermediate climate relative to the two extremes (**Table 1**). Based on flux

295 tower data collected over the last six years, the desert experienced the hottest air and soil
296 temperature (22.8±0.8 °C), received the least rainfall per annum (100±24 mm), and experienced
297 the greatest range of daily air and soil temperatures (10.8±0.4 and 10.9±0.2 °C, respectively), on
298 average. Plot-level temperature sensors indicated that from January to December of 2015, the
299 desert site was the hottest (29.3±0.4 °C), but the grassland was significantly hotter (22.0±0.4 °C)
300 than the scrubland (19.5±0.5 °C), which is consistent with elevation. In addition, over the course
301 of the study, the scrubland and grassland experienced the greatest diurnal temperature ranges
302 (26.2±0.5 and 24.8±0.4 °C, respectively) on average, and the subalpine site experienced the least
303 diurnal temperature variation (13.7±0.4 °C). Extrapolating the subalpine site's recent climate
304 from that observed at lower and higher elevations indicates that it has likely been the coldest site.
305
306 *3.2 Litter chemistry*
307 Relative fractions of cellulose, hemicellulose, lignin, crude protein, and structural and
308 non-structural carbohydrates are presented in **Table 2**. Litter chemistry was significantly affected
309 by site ($p<0.001$, $F_{4,24}=40.3$), season ($p<0.001$, $F_{1,6}=11.2$), and interactions between site and
310 season ($p<0.001$, $F_{4,24}=4.2$) (**Table 3**). In the dry season, structural carbohydrate content was
311 highest in the pine-oak and subalpine sites (34.0±0.3 and 31.3±0.5%), followed by the desert,
312 then the scrubland, and lowest in the grassland (13.3±0.8%). Crude protein content was greater
313 than 9% in the desert, scrubland, and grassland sites but less than 3% in the pine-oak and
314 subalpine sites. Cellulose content was highest in the desert and grassland sites (36.3±1.5 and
315 35.6±1.4%), and less than 30% in the scrubland, pine-oak, and subalpine sites. Non-structural
316 carbohydrate content was highest in the scrubland and pine-oak sites (12.6±0.5 and 10.5±0.3%),
317 intermediate in the grassland and subalpine sites, and lowest in the desert site (5.0±1.1%).

318 Site-level differences in litter chemistry followed similar trends in both the wet and dry
319 season for structural carbohydrate, cellulose, and protein content, but differed between seasons
320 for non-structural carbohydrate content. In the wet season, non-structural carbohydrate content
321 was greater than 11% in the scrubland, pine-oak, and subalpine sites, and ~5% in the desert and
322 grassland sites.

323 CDA showed that differences in the relative amounts of structural and non-structural
324 carbohydrates, cellulose, and protein explained most of the variation in litter chemistry both
325 between sites and between seasons (**Fig. S1**). When comparing differences in litter between sites,
326 the first CDA axis explained 91.1% of the variation, and the absolute values of loading
327 coefficients on this axis were 0.94, 0.93, 0.86, and 0.61 for fractions of structural carbohydrates,
328 crude protein, cellulose, and non-structural carbohydrates, respectively. When comparing
329 differences in litter between seasons, there was only one CDA axis, and the absolute values of
330 loading coefficients for crude protein, structural carbohydrates, cellulose, and non-structural
331 carbohydrates were 0.79, 0.78, 0.54, and 0.45, respectively.

332

333 *3.3 Microbial biomass*

334 Litter microbial biomass varied by site ($p<0.001$, $F_{4,44}=7.0$), season ($p<0.001$,
335 $F_{1,44}=133.5$), and their interaction ($p=0.002$, $F_{4,44}=4.9$) (**Table 3**). In the dry season (Oct. 2014),
336 microbial biomass was similar (0.37±0.02 mg C g^{-1} dry litter) in the scrubland, grassland, pine-
337 oak, and subalpine sites, and significantly lower (0.16±0.02 mg C g^{-1}) in the desert site (**Fig. 1A**).
338 In the wet season (Dec. 2015), microbial biomass was higher and more variable across the entire
339 gradient (**Fig. 1B**), and significantly higher in the grassland, pine-oak, and subalpine sites
340 (1.84±0.30 mg C g^{-1}) than in the desert and scrubland sites (0.79±0.10 mg C g^{-1}).

Litter fungal biomass varied by site ($p<0.001$, $F_{4,44}=34.0$) and season ($p=0.039$, $F_{1,44}=4.5$) (**Table 3**). In the dry season, fungal biomass was highest in the grassland site (0.24±0.02 mg C g^{-1}), intermediate in the scrubland and pine-oak sites (0.15±0.01), and lowest in the desert and subalpine sites (0.09±0.01) (**Fig. 1C**). Fungal biomass across sites increased from an average of 0.13±0.01 mg C g^{-1} in the dry season to an average of 0.15±0.01 in the wet season, likely because of increased fungal biomass in the grassland (**Fig. 1D**).

3.4 Potential extracellular enzyme activity

There was a significant effect of site on V_{max} ($p<0.001$, $F_{4,28}=28.2$), and a significant interaction between site and season ($p<0.001$, $F_{4,28}=6.6$) (**Table 3**). Mean V_{max} across all enzyme classes and seasons was highest in the grassland site, next-highest in the scrubland, intermediate in the desert, and lowest in the pine-oak and subalpine sites (Tukey $p<0.001$), with mean values of 24.2±2.0, 16.1±1.4, 10.6±0.7 and 3.3±0.3 $\mu mol \cdot hr^{-1} \cdot g^{-1}$, respectively (**Fig. 2**).

The first CDA axis explained >68% of the variance in V_{max}, and loading coefficients for all seven EE classes along the first axis were greater than 0.76 (**Fig. S2**). Therefore, V_{max} results were combined across enzyme classes for analyses of site-level differences.

There was no significant relationship between microbial biomass and mean V_{max} across the gradient (**Fig. S3A**), but there was a significant positive relationship between fungal biomass and mean V_{max} ($p<0.001$, $R^2=0.30$, **Fig. S3B**). Mean EE V_{max} and K_m values for all enzymes, sampling dates, and sites are presented in **Table S2**.

3.5 Potential extracellular enzyme half-saturation constant

There was a significant effect of site on K_m ($p<0.001$, $F_{4,28}=11.0$), and there was a significant interaction between site and season ($p<0.001$, $F_{4,28}=4.2$) (**Table 3**). Mean BG K_m across seasons was lowest in the subalpine site, intermediate in the desert site, and greatest in the scrubland, grassland, and pine-oak sites (Tukey $p<0.01$), with mean values of 106±13, 189±10, and 435±40 μM, respectively (**Fig. 3A**). Mean CBH K_m across seasons was also lowest in the subalpine site, intermediate in desert, scrubland, and pine-oak sites (Tukey $p<0.001$), and greatest in the grassland site, with mean values of 51±13, 100±8, and 273±25 μM, respectively (**Fig. 3B**). Mean LAP K_m across seasons was lowest in the desert, scrubland, and grassland sites and highest in the pine-oak and subalpine sites (Tukey $p<0.001$), with mean values of 183±15 and 560±110 μM, respectively (**Fig. 3C**). Mean NAG K_m across seasons was lowest in the desert, pine-oak, and subalpine sites, intermediate in the grassland site, and highest in the scrubland site (Tukey $p<0.05$), with mean values of 92±7, 171±13, and 289±64 μM, respectively (**Fig. 3D**).

The first CDA axis explained >58% of the cross-site variance in K_m, with cellobiohydrolase (CBH, |loading coefficient| = 0.87), β-glucosidase (BG, 0.82), and leucine aminopeptidase (LAP, 0.66) K_m distinguishing sites the most (**Fig. S4**). The second CDA axis explained >30% of the remaining cross-site variance in K_m, with N-acetyl-glucosaminidase (NAG, 0.86) K_m as the main response variable. As such, mean apparent K_m values across seasons for BG, CBH, LAP, and NAG were analyzed for site-level differences using pairwise comparisons.

There was no significant relationship between microbial biomass and mean K_m (**Fig. S5A**), but there was a significant positive relationship between fungal biomass and mean K_m ($p<0.001$, $R^2=0.12$, **Fig. S5B**). There was also a significant positive relationship between CBH

386 K_m and cellulose content and a negative relationship between LAP K_m and protein content across
387 sites and seasons, but there was no significant relationship between K_m and putative substrate
388 content for AG, BG, or BX (**Table 4**).
389
390 *3.6 Temperature sensitivity of V_{max}*
391 Temperature sensitivity of V_{max} was positive (Q_{10}>1) for all EE classes assayed at all
392 sites in both seasons (**Fig. 4A**). There were significant effects of site ($p<0.001$, $F_{4,28}=9.3$), season
393 ($p=0.001$, $F_{1,7}=4.4$), and the interaction between site and season ($p=0.007$, $F_{4,28}=2.0$) on observed
394 temperature sensitivity of EE V_{max} for all enzyme classes when analyzed in conjunction (**Table**
395 **3**). The temperature sensitivity-MAT relationship was significantly or marginally significantly
396 negative for six of the seven EE classes assayed in the wet season, but was only significant (and
397 positive) for LAP in the dry season (**Table 5**). The weak relationships during the dry season
398 generally resulted from lower EE temperature sensitivities in the coldest sites and higher
399 temperature sensitivities in the scrubland site when compared to the wet season. V_{max} Q_{10} values
400 for all enzymes assayed in all sites at all sampling dates are presented in **Table S3**.
401
402 *3.7 Temperature sensitivity of K_m*
403 Temperature sensitivity of K_m was positive for all EE classes assayed at all sites across
404 both seasons, except for AG in the subalpine site and LAP in the subalpine and pine-oak sites
405 (**Fig. 4B**). There were significant effects of site ($p<0.001$, $F_{4,20}=6.5$) on observed temperature
406 sensitivity of EE K_m of all enzyme classes when analyzed in conjunction, but no significant
407 effect of season or interaction between site and season (**Table 3**). Temperature sensitivity of K_m
408 exhibited a significant relationship with MAT across seasons for four of the EE classes assayed:

409 a positive relationship with LAP, BG, and NAG K_m (in order of increasing slope and
410 significance) and a negative relationship with BX K_m (**Table 5**). K_m Q_{10} values for all enzymes
411 assayed in all sites at all sampling dates are presented in **Table S4**.
412
413 **4. Discussion**
414 The gradient presented in this study spans five biomes in southern California along which
415 climate variables covary. Colder, wetter sites transition to hotter, drier sites in a manner that
416 emulates future climate change in the American Southwest. By analyzing litter along the
417 gradient, we determined that microbial communities differ in their EE kinetics in a manner
418 consistent with differences in fungal biomass, substrate availability, and proteolytic activity, but
419 not differences in total microbial biomass or local climate. We also observed that local microbial
420 communities occurring under different litter chemistry and long-term climate exhibit
421 significantly different EE temperature sensitivities. These sensitivities can be predicted in part by
422 local mean annual temperature. If climate is in fact what is driving these temperature
423 sensitivities, then as climate becomes more arid in the future, microbes at the wetter end of our
424 gradient will initially produce EEs that are relatively sensitive to increases in temperature.
425 However, as local climate transitions to more xeric conditions, the microbial communities will
426 potentially produce less temperature-sensitive EEs. In addition, systems undergoing the
427 transition to more xeric conditions will likely accumulate EEs that are mainly active during
428 increasingly episodic rainfall events (Alster et al., 2013).
429
430 *4.1 Climate and microbial activity*

We hypothesized that variations in microbial biomass in litter would be driven by differences in climate and substrate availability across the gradient, and that we would observe greater biomass in cooler, wetter sites. Our results did not support this hypothesis. Microbial biomass in both the dry season and wet season was similar in four of the five sites along the gradient despite significant differences in mean annual precipitation and air temperature (**Table 1**). Other research in Mediterranean and semiarid ecosystems indicates, however, that sporadic increases in water potential may actually inhibit microbial growth (Sherman et al., 2012), presumably because microbes adapted to semiarid conditions can experience severe osmotic stress when exposed to precipitation (Fierer and Schimel, 2003). High diurnal temperature variation and pulse-driven rainfall may therefore overwhelm any positive effects of increasing average precipitation on microbial growth in our sites.

We expected that microbial biomass would be related to both the production of enzymes (reflected in V_{max}) and the availability of substrates (as indicated by K_m) in litter along our gradient. Our results in part failed to support this hypothesis, as total microbial biomass did not explain a significant amount of the variation in mean V_{max} or K_m across sites at either time point (**Fig. S3A** and **S5A**). However, fungal biomass did explain a significant amount of the variation in mean V_{max} (**Fig. S3B**) and K_m (**Fig. S5B**) along the gradient, though this relationship was driven primarily by conjunction of high fungal biomass, V_{max}, and K_m in litter from the grassland site. Although both bacteria and fungi produce extracellular enzymes in decomposer communities, other studies have found evidence that fungi exert more control on community EE activity (Romaní et al., 2006) and that enzymes that degrade more complex polymers such as cellulose and lignin, in particular, are primarily produced by fungi rather than bacteria

453 (Schneider et al., 2012). Our results similarly indicate that fungal decomposers likely exert more
454 control than bacteria over EE production and potential decomposition rates along our gradient.
455 In general, mean V_{max} for the EE classes assayed in this study differed significantly by
456 site (**Table 3**), but the differences were not consistent with our initial hypothesis. Mean V_{max} of
457 all EEs in litter from the two highest elevation sites was an order of magnitude lower than in the
458 grassland, scrubland, and desert sites (**Fig. 2**), even though the three lower elevation sites receive
459 less precipitation and have drier soils (**Table 1**). Rather than climate-driven production of
460 enzymes, our results suggest that EE V_{max} may be driven by enzyme turnover. The subalpine
461 and pine-oak litter showed low levels of crude protein (**Table 2**) but high K_m values for
462 proteolytic enzyme (LAP; **Fig. 3**), which could imply a greater abundance of protein degradation
463 products (Chróst, 1990). If so, protein turnover may be occurring more rapidly in these sites,
464 thereby reducing enzyme V_{max}.
465 Our results for microbial biomass and EE V_{max} are consistent with those of a prior study
466 performed in the grassland site along our gradient. Alster et al. (2013) found that increases in
467 microbial biomass over the wet season did not correspond with increases in EE V_{max}, and that EE
468 V_{max} remained static from the end of the wet season to the middle of the dry season, despite
469 significant reductions in microbial biomass. These EE dynamics can be explained in part by the
470 observation that proteolytic EEs were the only enzyme class to decline in V_{max} under drought.
471 Reduced proteolytic activity may allow EEs in arid and semiarid ecosystems to persist long after
472 their production by ephemeral microbial decomposers, a mechanism supported by our LAP K_m
473 and crude protein results at some sites along our gradient.
474 Our enzyme and protein accumulation results may help explain pulses of CO_2 that are
475 emitted by microbial communities in Mediterranean ecosystems, particularly grasslands, when

476 exposed to rewetting after long dry periods. EEs persisting in microsites may degrade substrate
477 during periods of elevated humidity or at dewpoint, resulting in accumulation of labile substrates
478 during dry periods. After rewetting, these labile compounds combine with built up microbial
479 necromass (Blazewicz et al., 2014) and soil organic matter released from aggregates (Fierer and
480 Schimel, 2003) to produce large pulses of CO_2 (Zhang et al., 2014).
481
482 *4.2 Temperature sensitivity of EE kinetics*
483 The results of our study support a growing consensus that EE kinetic parameters have
484 positive temperature sensitivities (German et al., 2012; Lehmeier et al., 2013; Min et al., 2014;
485 Stone et al., 2011). We show that these results hold true for EEs in litter, a substrate for which
486 such intrinsic responses to temperature have rarely been explored (but see Bárta et al. 2014). Our
487 hypothesis that cold-adapted EEs would have reduced V_{max} temperature sensitivity compared to
488 warm-adapted enzymes was not supported for EEs in either season – instead, the opposite trend
489 of cold-adapted enzymes exhibiting greater V_{max} temperature sensitivity was observed in the wet
490 season (but not the dry season). Significant relationships between temperature sensitivity of EE
491 V_{max} and MAT in the wet season were driven by a bimodal trend, whereby the two high
492 elevation, forested sites had higher temperature sensitivities, and the three lower elevation, grass
493 and scrub-dominated sites had significantly lower temperature sensitivities (**Fig. 4A**). During the
494 dry season, this bimodal trend disappeared as the two higher elevation sites no longer exhibited
495 higher temperature sensitivity of EE V_{max} in comparison with the lower elevation sites. This
496 indicates that the structure of enzymes produced by microbial decomposer communities along
497 this gradient vary seasonally, likely as a result of different organisms being responsible for
498 producing those enzymes at different times of year (Wallenstein and Weintraub, 2008).

499 Previous studies have shown seasonal variation in EE temperature sensitivity of V_{max}
500 (Brzostek and Finzi, 2012; Fenner et al., 2005; Koch et al., 2007; Trasar-Cepeda et al., 2007;
501 Wallenstein et al., 2009) and others have shown site-to-site variation in temperature sensitivity of
502 V_{max} (German et al., 2012; Khalili et al., 2011; Stone et al., 2011). Some of these studies
503 indicate that EEs from colder biomes or seasons exhibit greater temperature sensitivity (Koch et
504 al., 2007; Wallenstein et al., 2009), in contrast with thermodynamic theory but in agreement with
505 our findings. A previous study of EE V_{max} temperature sensitivity in soils across a latitudinal
506 gradient found no relationship between site MAT and temperature sensitivities for all but one EE
507 class (German et al., 2012). However, this study did not control for season when collecting soils,
508 and our results indicate that ignoring seasonality may obscure potentially significant
509 relationships between site MAT and EE thermodynamics.
510 In contrast with our V_{max} results, our hypothesis that K_m of cold-adapted EEs would show
511 reduced temperature sensitivity was supported by our results. There are indications that K_m
512 temperature sensitivity exhibits a significant positive relationship with MAT, as BG, LAP, and
513 NAG K_m temperature sensitivities were generally higher in hotter sites. It is possible that
514 environmental variables other than mean annual temperature play a greater role in determining
515 EE K_m temperature sensitivities – all major climatic variables were correlated along our gradient,
516 so an apparent response to MAT could also be linked to MAP, solar radiation, or biotic factors
517 that covary with climate. V_{max} temperature sensitivity also exceeded K_m temperature sensitivity
518 for all EEs, at all sites, in both seasons. Therefore, it is possible that temperature effects on V_{max}
519 outweigh those on K_m, both in lab assays and in response to natural selection. To our knowledge,
520 this is the first study of seasonal variation in K_m temperature sensitivity, though we did not
521 observe significant seasonal variation in this EE parameter.

522

523 *4.3 Conclusions*

524 Our study shows that EE kinetics in southern California are not explained by total
525 microbial biomass, but may be more dependent on fungal biomass. In addition, potential
526 interactions between substrate availability and proteolytic activity likely drive observed EE
527 kinetics along this gradient. Accumulation of EE relative to substrate in the more arid sites along
528 our gradient may partially explain the pulses of CO_2 emitted during rewetting events after the dry
529 season, as EEs remain present while microbial biomass declines over the course of the dry
530 season.

531 As the American Southwest shifts to a more arid climate in the future, biomes will shift
532 towards the hotter, drier end of our gradient. Our results indicate that litter will become more
533 cellulosic and contain more protein – likely as a result of increased accumulation of EEs
534 produced by litter-bound microbial communities. These shifts will increase the influence of
535 rewetting events, making resource pulses more episodic and potentially more difficult to predict.
536 The EEs produced by these communities may initially be very sensitive to temperature,
537 particularly in subalpine and montane forests, but our results indicate that over time EEs
538 produced by these communities may become less sensitive to climate as microbes adapted to
539 hotter, drier conditions become more prevalent.

540 Our study also shows that the temperature sensitivity of EE kinetics varies seasonally,
541 and that large-scale climate indices can explain variation in EE temperature sensitivities in the
542 wet season, but not in the dry season. When taken in conjunction with evidence of extracellular
543 enzyme accumulation across our gradient, our temperature sensitivity results suggest two lines of
544 research for the next generation of carbon-cycling models that explicitly account for enzymatic

545 decomposition (Sihi et al., 2015; Sulman et al., 2014; Wieder et al., 2014). First, if EE potential
546 in arid and semiarid systems indicates enzyme accumulation, not just activity, then we must
547 determine when enzymes are seasonally most active to parameterize C-cycling models. Second,
548 we must determine temperature sensitivities of EE kinetics during the seasons when EEs are
549 most active to predict how enzyme-driven decomposition will be affected by future changes in
550 temperature.
551

552 **5. Acknowledgements**

553 Funding for this project was provided by the U.S. National Science Foundation's Ecosystem
554 Studies Program, as well as a U.C.N.R.S. Mathias Grant. We thank J. Gee and J.W. Laundre of
555 the James Reserve, A. Muth of the Boyd Deep Canyon Desert Research Center, J. Burger of the
556 Irvine Ranch Conservancy, and J. Ladley of the San Bernardino National Forest Service for their
557 support in making use of land under their management. We thank J.B.H. Martiny and A.C.
558 Martiny for helpful discussion and comments. We thank D.E. Islip, G.A. Barajas, E. Stogner,
559 M.Y. Farah, and, in particular, D.M. Nisson for their hours of dedicated service on this project.

Table 1 Mean (± SE) historic annual climate parameters and native litter types for the five sites used in this study, and plot-level temperature over the course of one year encompassing both sampling dates.

Variable	Desert	Scrubland	Grassland	Pine-Oak	Subalpine	Period
Air temperature (°C)	22.8±0.8	15.6±0.8	16.4±0.3	12.3±0.6	*10.3±1.8*	2009-14
Air daily temp. range	10.8±0.4	8.5±0.2	8.3±0.3	6.2±0.2	-	2009-14
Soil temperature (°C)	28.3±0.3	18.4±0.3	19.1±0.9	9.9±0.3	-	2008-12
Soil daily temp. range	10.9±0.2	5.5±0.7	4.6±0.8	2.6±0.1	-	2008-12
Plot temperature (°C)	29.3±0.4	19.5±0.5	22.0±0.4	13.2±0.4	11.5±0.4	2015
Plot daily temp. range	20.3±0.3	24.8±0.4	26.2±0.5	20.8±0.5	13.7±0.4	2015
Rainfall (mm)	100±24	193±33	242±76	402±118	*~265*	2009-14
Soil moisture (g/cm^3)	4.6±0.1	7.3±0.5	7.3±0.8	8.6±0.3	-	2008-12
Solar radiation (W/m^2)	225±7	234±7	217±8	224±7	*~270*	2006-13
Elevation (m)	275	1280	470	1710	2250	
Dominant litter type	Grasses, shrub leaves	Grasses, needles, shrub leaves	Grasses, forb leaves	Needles, tree leaves	Needles, tree leaves	

Table 2 Mean (± SE) percentage of non-ash dry weight of litter attributed to cellulose, hemicellulose, lignin, crude protein, structural carbohydrates, and non-structural carbohydrates, in all five sites during the dry season (June 2015) and the wet season (December 2015).

Dry season (June 2015)					
Compound	**Desert**	**Scrubland**	**Grassland**	**Pine-Oak**	**Subalpine**
Cellulose	35.6±1.4	28.0±0.7	36.3±1.5	24.1±0.4	24.1±0.7
Hemicellulose	0.0	17.1±2.7	16.0±2.3	5.6±0.2	6.1±0.3
Lignin	17.4±0.6	8.0±0.7	8.0±0.4	13.6±0.1	13.8±0.5
Crude protein	9.1±0.8	12.8±0.9	11.9±0.9	1.9±0.2	2.9±0.5
Struct. Carbs.	25.7±0.9	17.2±1.7	13.3±0.8	31.3±0.5	34.0±0.3
Non-struct. Carbs.	5.0±1.1	10.5±0.3	8.8±1.6	12.6±0.5	8.9±0.9
Wet season (December 2015)					
Compound	**Desert**	**Scrubland**	**Grassland**	**Pine-Oak**	**Subalpine**
Cellulose	33.1±0.5	27.6±4.3	36.0±1.0	22.2±0.7	23.1±0.5
Hemicellulose	0.9±0.4	20.9±0.2	8.6±1.9	5.3±0.7	5.5±1.1
Lignin	16.2±0.1	8.2±0.3	14.3±0.7	13.1±0.7	13.9±0.8
Crude protein	11.0±0.2	14.9±2.6	16.5±1.1	1.5±0.3	2.8±0.7
Struct. Carbs.	18.7±0.4	12.0±0.1	12.6±0.9	30.6±0.4	32.8±0.7
Non-struct. Carbs.	4.9±0.2	11.0±0.7	5.1±0.8	16.0±0.8	11.6±1.3

561

Table 3 The p-values for independent variables from ANCOVA ([A]) or MANCOVA ([M]), run with gravimetric litter moisture (H_2O) as a covariate. Significant (<0.05) p-values are in bold. "Normality" indicates the type of transformation required to normalize the data by the indicated method. Visual tests of adherence to normality were performed using quartile-quartile plots of residuals.

Response variable	Site	Season	Site:Season	H_2O	Normality
Microbial biomass [A]	**<0.001**	**<0.001**	**0.002**	0.106	Log, test
Fungal biomass [A]	**<0.001**	**0.039**	0.107	0.527	Log, test
Litter chemistry [M]	**<0.001**	**<0.001**	**<0.001**	0.694	Base, visual
Vmax [M]	**<0.001**	0.227	**<0.001**	**<0.001**	Log, visual
Km [M]	**<0.001**	0.114	**<0.001**	**0.004**	Log, visual
Vmax TS [M]	**<0.001**	**0.001**	**<0.001**	0.051	Base, visual
Km TS [M]	**<0.001**	0.628	0.104	0.510	Base, visual

562

Table 4 Pearson coefficients and p-values for the correlation between EE K_m and percentage of litter mass attributed to the substrate degraded by that EE class. R^2 values for the linear regression between the two variables are presented for significant relationships.

Enzyme	Substrate	Correlation	R^2	p
α-glucosidase	Starches	0.12	-	0.383
β-glucosidase	Cellulose	-0.14	-	0.312
β-xylosidase	Hemicellulose	0.18	-	0.193
Cellobiohydrolase	Cellulose	0.60	0.35	**<0.001**
Leucine aminopeptidase	Protein	-0.60	0.35	**<0.001**

563

Table 5 Slope (± SE), R^2, and p-values for linear regression of EE V_{max} and K_m Q_{10} against site mean annual temperature for each EE class by site and season. Bolded p-values are significant (<0.05).

	Vmax, dry season			Vmax, wet season			Km, both seasons		
Enzyme	Slope	R^2	p	Slope	R^2	p	Slope	R^2	p
AG	0.019±0.025	-	0.450	-0.080±0.040	0.08	0.053	-0.004±0.024	-	0.879
AP	-0.001±0.005	-	0.766	-0.023±0.005	0.41	**<0.001**	-0.005±0.005	-	0.318
BG	-0.005±0.011	-	0.649	-0.028±0.008	0.27	**0.002**	0.039±0.007	0.39	**<0.001**
BX	-0.017±0.016	-	0.279	-0.094±0.025	0.30	**<0.001**	-0.057±0.014	0.27	**<0.001**
CBH	-0.030±0.032	-	0.351	-0.097±0.030	0.24	**0.004**	-0.013±0.014	-	0.368
LAP	0.023±0.010	0.15	**0.028**	-0.018±0.030	-	0.530	0.084±0.014	0.62	**<0.001**
NAG	-0.010±0.008	-	0.261	-0.039±0.012	0.25	**0.003**	0.012±0.005	0.09	**0.013**

564

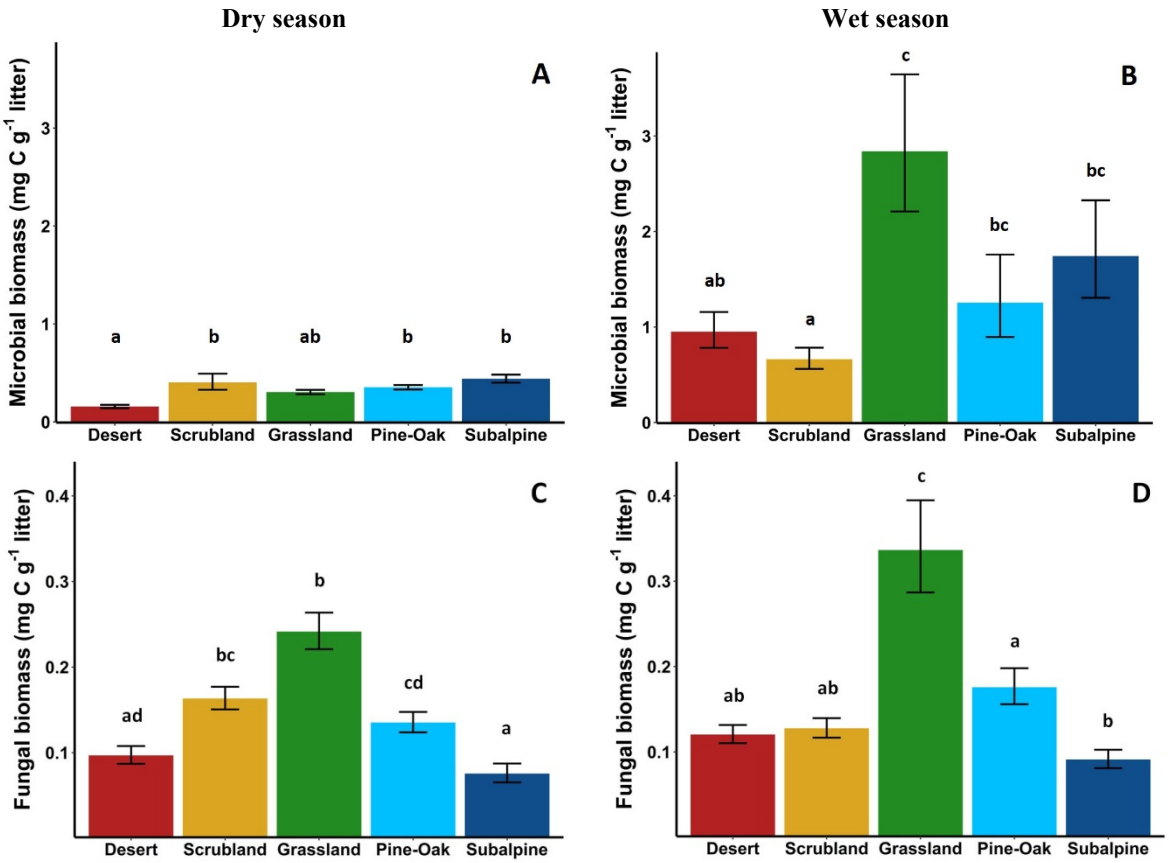

Figure 1 Mean microbial biomass by site in mg C g^{-1} dry litter in **A)** October 2014 and **B)** December 2015, and mean fungal biomass in **C)** October 2014 and **D)** December 2015 (n=6 for each site). Error bars denote standard error. Depicted means and standard errors are back-transformed from ln values. Means sharing the same letter are not statistically different ($p>0.05$).

565

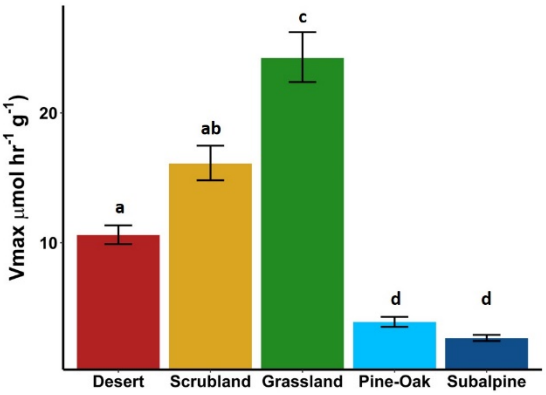

Figure 2 Mean EE V_{max} in µmol hr^{-1} g^{-1} across all enzyme classes and both seasons (n=12 for each site). Error bars denote standard error. Depicted means and standard errors are back-transformed from ln values. Means sharing the same letter are not statistically different ($p>0.05$).

566

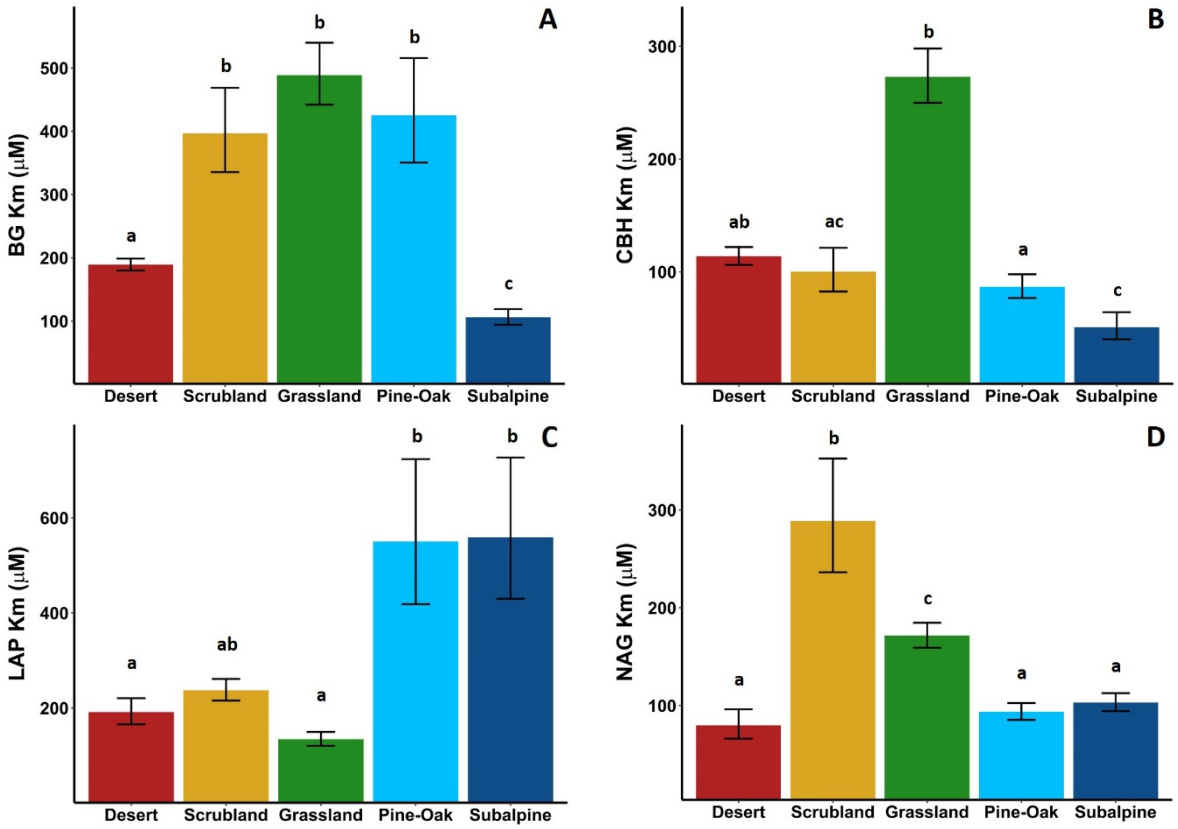

Figure 3 Mean EE K_m in μM across seasons for the four EE classes whose K_m most distinguished sites from one another: **A**) BG, **B**) CBH, **C**) LAP, and **D**) NAG (n=12 for each site). Error bars denote standard error. Depicted means and standard errors have been back-transformed from ln K_m values. Means sharing the same letter are not statistically different ($p>0.05$)

567

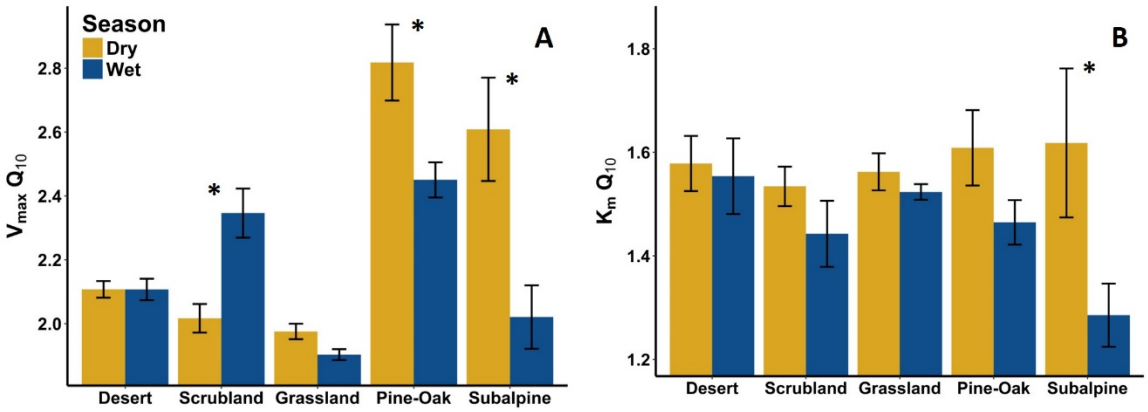

Figure 4 Mean Q_{10} across all enzymes by site in the dry season (June 2015) and wet season (December 2015) for **A)** V_{max} and **B)** K_m. Note that the y-axis scale differs between the two plots. Error bars denote standard error. Asterisks (*) denote significant differences between mean EE Q_{10} in the dry season vs. the wet season (Tukey $p<0.05$).

568

References

Allison, S.D., Gartner, T.B., Holland, K., Weintraub, M., Sinsabaugh, R.L., 2007. Soil enzymes: linking proteomics and ecological process, in: Manual of Environmental Microbiology. ASM Press, pp. 704–711.

Allison, S.D., Lu, Y., Weihe, C., Goulden, M.L., Martiny, A.C., Treseder, K.K., Martiny, J.B.H., 2013. Microbial abundance and composition influence litter decomposition response to environmental change. Ecology 94, 714–25.

Alster, C.J., German, D.P., Lu, Y., Allison, S.D., 2013. Microbial enzymatic responses to drought and to nitrogen addition in a southern California grassland. Soil Biology and Biochemistry 64, 68–79. doi:10.1016/j.soilbio.2013.03.034

Bárta, J., Šlajsová, P., Tahovská, K., Picek, T., Šantrůčková, H., 2014. Different temperature sensitivity and kinetics of soil enzymes indicate seasonal shifts in C, N and P nutrient stoichiometry in acid forest soil. Biogeochemistry 117, 525–537. doi:10.1007/s10533-013-9898-1

Blazewicz, S.J., Schwartz, E., Firestone, M.K., 2014. Growth and death of bacteria and fungi underlie rainfall-induced carbon dioxide pulses from seasonally dried soil. Ecology 95, 1162–1172. doi:10.1890/13-1031.1

Bratbak, G., 1985. Bacterial biovolume and biomass estimations. Applied and Environmental Microbiology 49, 1488–1493.

Brzostek, E.R., Finzi, A.C., 2012. Seasonal variation in the temperature sensitivity of proteolytic enzyme activity in temperate forest soils. Journal of Geophysical Research: Biogeosciences 117, 1–10. doi:10.1029/2011JG001688

Burns, R.G., DeForest, J.L., Marxsen, J., Sinsabaugh, R.L., Stromberger, M.E., Wallenstein,

M.D., Weintraub, M.N., Zoppini, A., 2013. Soil enzymes in a changing environment: Current knowledge and future directions. Soil Biology and Biochemistry 58, 216–234. doi:10.1016/j.soilbio.2012.11.009

Chróst, R.J., 1990. Microbial ectoenzymes in aquatic environments, in: Aquatic Microbial Ecology. Springer, New York, pp. 47–78.

Davidson, E.A., Janssens, I.A., 2006. Temperature sensitivity of soil carbon decomposition and feedbacks to climate change. Nature 440, 165–73. doi:10.1038/nature04514

Davidson, E.A., Janssens, I.A., Luo, Y., 2006. On the variability of respiration in terrestrial ecosystems: moving beyond Q10. Global Change Biology 12, 154–164. doi:10.1111/j.1365-2486.2005.01065.x

Fenner, N., Freeman, C., Reynolds, B., 2005. Observations of a seasonally shifting thermal optimum in peatland carbon-cycling processes; implications for the global carbon cycle and soil enzyme methodologies. Soil Biology & Biochemistry 37, 1814–1821. doi:10.1016/j.soilbio.2005.02.032

Fierer, N., Schimel, J.P., 2003. A Proposed Mechanism for the Pulse in Carbon Dioxide Production Commonly Observed Following the Rapid Rewetting of a Dry Soil. Soil Science Society of America Journal 67, 798–805. doi:10.2136/sssaj2003.0798

Garfin, G., Franco, G., Blanco, H., Comrie, A., Gonzalez, P., Piechota, T., Smyth, R., Waskom, R., 2014. Climate Change Impacts in the United States: The Third National Climate Assessment, in: Melillo, J., TC, R., Yohe, G. (Eds.), . U.S. Global Climate Change Research Program, pp. 462–486. doi:10.7930/J08G8HMN.On

Georlette, D., Blaise, V., Collins, T., D'Amico, S., Gratia, E., Hoyoux, A., Marx, J.C., Sonan, G., Feller, G., Gerday, C., 2004. Some like it cold: biocatalysis at low temperatures. FEMS

615 Microbiology Reviews 28, 25–42. doi:10.1016/j.femsre.2003.07.003
616 German, D.P., Marcelo, K.R., Stone, M.M., Allison, S.D., 2012. The Michaelis-Menten kinetics
617 of soil extracellular enzymes in response to temperature: a cross-latitudinal study. Global
618 Change Biology 18, 1468–1479. doi:10.1111/j.1365-2486.2011.02615.x
619 German, D.P., Weintraub, M.N., Grandy, a. S., Lauber, C.L., Rinkes, Z.L., Allison, S.D., 2011.
620 Optimization of hydrolytic and oxidative enzyme methods for ecosystem studies. Soil
621 Biology and Biochemistry 43, 1387–1397. doi:10.1016/j.soilbio.2011.03.017
622 Goulden, M.L., Winston, G.C., Mcmillan, A.M., Litvak, M.E., Read, E.L., Rocha, A. V, Elliot,
623 J.R., 2006. An eddy covariance mesonet to measure the effect of forest age on land-
624 atmosphere exchange. Global Change Biology 12, 2146–2162. doi:10.1111/j.1365-
625 2486.2006.01251.x
626 IPCC, 2014. Climate Change 2014: Synthesis Report. Contribution of Working Groups I, II and
627 III to the Fifth Assessment Report of the Intergovernmental Panel on Climate Change [Core
628 Writing Team, R.K. Pachauri and L.A. Meyer (eds.)]. Geneva, Switzerland.
629 Johns, G.C., Somero, G.N., 2004. Evolutionary Convergence in Adaptation of Proteins to
630 Temperature: A4-Lactate Dehydrogenases of Pacific Damselfishes (Chromis spp.).
631 Molecular Biology and Evolution 21, 314–320. doi:10.1093/molbev/msh021
632 Khalili, B., Nourbakhsh, F., Nili, N., Khademi, H., Sharifnabi, B., 2011. Diversity of soil
633 cellulase isoenzymes is associated with soil cellulase kinetic and thermodynamic
634 parameters. Soil Biology and Biochemistry 43, 1639–1648.
635 doi:10.1016/j.soilbio.2011.03.019
636 Kivlin, S.N., Hawkes, C. V., Treseder, K.K., 2011. Global diversity and distribution of
637 arbuscular mycorrhizal fungi. Soil Biology and Biochemistry 43, 2294–2303.

638 doi:10.1016/j.soilbio.2011.07.012
639 Koch, O., Tscherko, D., Kandeler, E., 2007. Temperature sensitivity of microbial respiration,
640 nitrogen mineralization, and potential soil enzyme activities in organic alpine soils. Global
641 Biogeochemical Cycles 21, 1–11. doi:10.1029/2007GB002983
642 Lehmeier, C.A., Min, K., Niehues, N.D., Ballantyne, F., Billings, S.A., 2013. Temperature-
643 mediated changes of exoenzyme-substrate reaction rates and their consequences for the
644 carbon to nitrogen flow ratio of liberated resources. Soil Biology and Biochemistry 57,
645 374–382. doi:10.1016/j.soilbio.2012.10.030
646 Lonhienne, T., Gerday, C., Feller, G., 2000. Psychrophilic enzymes: revisiting the
647 thermodynamic parameters of activation may explain local flexibility. Biochimica et
648 Biophysica Acta - Protein Structure and Molecular Enzymology 1543, 1–10.
649 doi:10.1016/S0167-4838(00)00210-7
650 MEA, 2005. Ecosystems and Human Well-Being: Desertification Synthesis, in: Millenium
651 Ecosystem Assessment. World Resources Institute, Washington, DC. doi:ISBN: 1-56973-
652 590-5
653 Min, K., Lehmeier, C., Ballantyne, F., Tatarko, A., Billings, S.A., 2014. Differential effects of
654 pH on temperature sensitivity of organic carbon and nitrogen decay. Sbb 76, 193–200.
655 Paul, E.A., Clark, F.E., 1996. Components of the Soil Biota, in: Soil Microbiology and
656 Biochemistry. Academic Press, San Diego.
657 R Development Core Team, 2016. R: A Language and Environment for Statistical Computing. R
658 Foundation for Statistical Computing.
659 Raich, J.W., Schlesinger, W.H., 2002. The global carbon dioxide flux in soil respiration and its
660 relationship to vegetation and climate. Tellus 44, 81–99.

661 Romaní, A.M., Fischer, H., Mille-Lindblom, C., Tranvik, L.J., 2006. Interactions of Bacteria and
662 Fungi on Decomposing Litter: Differential Extracellular Enzyme Activities. Ecology 87,
663 2559–2569.
664 Saleska, S.R., Shaw, M.R., Fischer, M.L., Dunne, J. a., Still, C.J., Holman, M.L., Harte, J., 2002.
665 Plant community composition mediates both large transient decline and predicted long-term
666 recovery of soil carbon under climate warming. Global Biogeochemical Cycles 16, 3-1-3–
667 18. doi:10.1029/2001GB001573
668 Schimel, J.P., Schaeffer, S.M., 2012. Microbial control over carbon cycling in soil. Frontiers in
669 Microbiology 3, 348. doi:10.3389/fmicb.2012.00348
670 Schneider, T., Keiblinger, K.M., Schmid, E., Sterflinger-Gleixner, K., Ellersdorfer, G.,
671 Roschitzki, B., Richter, A., Eberl, L., Zechmeister-Boltenstern, S., Riedel, K., 2012. Who is
672 who in litter decomposition? Metaproteomics reveals major microbial players and their
673 biogeochemical functions. The ISME Journal 6, 1749–62. doi:10.1038/ismej.2012.11
674 Seager, R., Ting, M., Held, I., Kushnir, Y., Lu, J., Vecchi, G., Huang, H.-P., Harnik, N.,
675 Leetmaa, A., Lau, N.-C., Li, C., Velez, J., Naik, N., 2007. Model projections of an
676 imminent transition to a more arid climate in southwestern North America. Science 316,
677 1181–1184. doi:10.1126/science.1139601
678 Shepherd, K.D., Vanlauwe, B., Gachengo, C.N., Palm, C. a., 2005. Decomposition and
679 mineralization of organic residues predicted using near infrared spectroscopy. Plant and Soil
680 277, 315–333. doi:10.1007/s11104-005-7929-y
681 Sherman, C., Sternberg, M., Steinberger, Y., 2012. Effects of climate change on soil respiration
682 and carbon processing in Mediterranean and semi-arid regions: An experimental approach.
683 European Journal of Soil Biology 52, 48–58. doi:10.1016/j.ejsobi.2012.06.001

684 Siddiqui, K.S., Cavicchioli, R., 2006. Cold-Adapted Enzymes. Annual Review of Biochemistry
685 75, 403–433. doi:10.1146/annurev.biochem.75.103004.142723
686 Sihi, D., Gerber, S., Inglett, P., Inglett, K., 2015. Comparing models of microbial-substrate
687 interactions and their response to warming. Biogeosciences Discussions 12, 10857–10897.
688 doi:10.5194/bgd-12-10857-2015
689 Sinsabaugh, R., Moorhead, D., Linkins, A., 1994. The enzymic basis of plant litter
690 decomposition: emergence of an ecological process. Applied Soil Ecology 1, 97–111.
691 Sinsabaugh, R.L., Belnap, J., Findlay, S.G., Shah, J.J.F., Hill, B.H., Kuehn, K.A., Kuske, C.R.,
692 Litvak, M.E., Martinez, N.G., Moorhead, D.L., Warnock, D.D., 2014. Extracellular enzyme
693 kinetics scale with resource availability. Biogeochemistry 121, 287–304.
694 doi:10.1007/s10533-014-0030-y
695 Sinsabaugh, R.L., Lauber, C.L., Weintraub, M.N., Ahmed, B., Allison, S.D., Crenshaw, C.,
696 Contosta, A.R., Cusack, D., Frey, S., Gallo, M.E., Gartner, T.B., Hobbie, S.E., Holland, K.,
697 Keeler, B.L., Powers, J.S., Stursova, M., Takacs-Vesbach, C., Waldrop, M.P., Wallenstein,
698 M.D., Zak, D.R., Zeglin, L.H., 2008. Stoichiometry of soil enzyme activity at global scale.
699 Ecology Letters 11, 1252–64. doi:10.1111/j.1461-0248.2008.01245.x
700 Sinsabaugh, R.L., Shah, J., 2011. Ecoenzymatic stoichiometry of recalcitrant organic matter
701 decomposition: the growth rate hypothesis in reverse. Biogeochemistry 102, 31–43.
702 doi:10.1007/s10533-010-9482-x
703 Sørensen, T.H., Cruys-Bagger, N., Windahl, M.S., Badino, S.F., Borch, K., Westh, P., 2015.
704 Temperature Effects on Kinetic Parameters and Substrate Affinity of Cel7A
705 Cellobiohydrolases 290, 22193–22202. doi:10.1074/jbc.M115.658930
706 Stone, M.M., Weiss, M.S., Goodale, C.L., Adams, M.B., Fernandez, I.J., German, D.P., Allison,

S.D., 2011. Temperature sensitivity of soil enzyme kinetics under N-fertilization in two temperate forests. Global Change Biology 18, 1173–1184. doi:10.1111/j.1365-2486.2011.02545.x

Sulman, B.N., Phillips, R.P., Oishi, A.C., Shevliakova, E., Pacala, S.W., 2014. Microbe-driven turnover offsets mineral-mediated storage of soil carbon under elevated CO2. Nature Climate Change 4, 1099–1102. doi:10.1038/nclimate2436

Sylvia, D.M., 1992. Quantification of external hyphae of vesicular-arbuscular mycorrhizal fungi. Methods in Microbiology 24, 53–65.

Trasar-Cepeda, C., Gil-Sotres, F., Leirós, M., Press, A.I.N., Trasar-Cepeda, C., Gil-Sotres, F., Leirós, M., 2007. Thermodynamic parameters of enzymes in grassland soils from Galicia, NW Spain. Soil Biology & Biochemistry 39, 311–319. doi:10.1016/j.soilbio.2006.08.002

Wallenstein, M., Allison, S.D., Ernakovich, J., Steinweg, M.J., Sinsabaugh, R., 2011. Controls on the temperature sensitivity of soil enzymes, in: Shukla, G., Varma, A. (Eds.), Soil Enzymology, Soil Biology. Springer Berlin Heidelberg, Berlin, Heidelberg, pp. 245–258. doi:10.1007/978-3-642-14225-3

Wallenstein, M.D., Mcmahon, S.K., Schimel, J.P., Resource, N., Collins, F., Barbara, S., 2009. Seasonal variation in enzyme activities and temperature sensitivities in Arctic tundra soils. Global Change Biology 15, 1631–1639. doi:10.1111/j.1365-2486.2008.01819.x

Wallenstein, M.D., Weintraub, M.N., 2008. Emerging tools for measuring and modeling the in situ activity of soil extracellular enzymes. Soil Biology and Biochemistry 40, 2098–2106. doi:10.1016/j.soilbio.2008.01.024

Whitford, W.G., Meentemeyer, V., Seastedt, T.R., Cromack, K., Crossley, D.A., Santos, P., Todd, R.L., Waide, J.B., 1981. Exceptions to the AET model: deserts and clear-cut forest.

730 Ecology 62, 275–277.
731 Wieder, W.R., Grandy, A.S., Kallenbach, C.M., Bonan, G.B., 2014. Integrating microbial
732 physiology and physio-chemical principles in soils with the MIcrobial-MIneral Carbon
733 Stabilization (MIMICS) model. Biogeosciences 11, 3899–3917. doi:10.5194/bg-11-3899-
734 2014
735 Zhang, X., Niu, G.Y., Elshall, A.S., Ye, M., Barron-Gafford, G.A., Pavao-Zuckerman, M., 2014.
736 Assessing five evolving microbial enzyme models against field measurements from a
737 semiarid savannah - What are the mechanisms of soil respiration pulses? Geophysical
738 Research Letters 41, 6428–6434. doi:10.1002/2014GL061399
739

SUPPLEMENTAL INFORMATION

Table S1. Enzymes, substrates, and substrate concentrations used in this study. Substrate concentrations refer to those used in the actual assays, with eight concentrations (max concentration + seven serial half-dilutions) being used from within each range.

Enzyme	Putative substrate	Synthetic substrate	[Substrate]
α-glucosidase (AG)	Starch degradation products	4-MUB-*α*-D-glucopyranoside	1.5625-200 µM
Acid phosphatase (AP)	Organic P	4-MUB Phosphate	6.25-800 µM
β-glucosidase (BG)	Cellulose degradation products	4-MUB-*β*-D-glucopyranoside	3.125-400 µM
β-xylosidase (BX)	Hemicellulose degradation products	4-MUB-*β*-D-xylopyranoside	3.125-400 µM
Cellobiohydrolase (CBH)	Cellulose degradation products	4-MUB-*β*-D-cellobioside	1.5625-200 µM
Leucine-aminopeptidase (LAP)	Peptide terminals	L-leucine-7-amido-4-methylcoumarin hydrochloride	1.5625-200 µM
N-acetyl-*β*-D-glucosaminidase (NAG)	Chitin degradation products	4-MUB-*N*-acetyl-*β*-D-glucosaminide	3.125-400 µM

Table S2. Mean (± SE) V_{max} (μmol·hr^{-1}·g^{-1}) and K_m (μM) for all enzyme classes in each site at all sampling dates.

		Vmax			Km		
Enzyme	Site	Oct. 2014	Jun. 2015	Dec. 2015	Oct. 2014	Jun. 2015	Dec. 2015
α-glucosidase (AG)	Desert	0.8±0.0	0.9±0.1	0.9±0.0	156.5±5.4	205±28	208.7±7.4
	Scrubland	1.0±0.0	0.4±0.1	2.2±0.3	227±11	197±46	273±13
	Grassland	1.7±0.1	2.4±0.2	4.0±0.2	267±11	247±19	231±10
	Forest	0.1±0.0	0.3±0.0	0.1±0.0	240±86	212±29	280±110
	Subalpine	0.2±0.0	0.4±0.1	0.4±0.1	520±150	197±32	297±90
Acid phosphatase (AP)	Desert	18.5±0.6	23.7±4.0	13.7±0.3	402±10	426±39	373±17
	Scrubland	22.9±0.5	54.6±1.9	40.9±4.5	372.7±7.3	466±10	459±31
	Grassland	38.9±1.0	24.1±1.6	24.5±5.6	480±21	306±18	394±73
	Forest	9.0±0.2	8.9±0.5	11.5±1.2	475±20	541±40	588±29
	Subalpine	9.6±0.1	5.8±0.5	9.2±0.7	277±11	479±55	451±17
β-glucosidase (BG)	Desert	22.0±0.4	25.6±2.1	22.3±0.5	170.5±3.9	180±14	199±11
	Scrubland	23.7±0.3	13.0±2.3	37.2±7.0	303.9±8.4	490±120	319±42
	Grassland	52.3±1.3	80.8±6.5	42.9±9.0	531±21	609±42	392±51
	Forest	5.9±0.1	8.3±1.3	10.3±1.9	265.2±9.2	232±26	703±83
	Subalpine	4.6±0.2	5.2±0.6	6.0±1.2	199±13	88±13	127±18
β-xylosidase (BX)	Desert	10.78±0.37	13.3±1.5	9.35±0.48	549±41	496±23	602±50
	Scrubland	9.82±0.47	2.32±0.76	16.8±3.9	586±46	390±67	548±49
	Grassland	39.6±1.2	18.3±1.4	14.8±2.0	571±19	508±12	468±20
	Forest	0.8±0.1	2.1±0.4	1.1±0.2	391±33	871±28	560±120
	Subalpine	0.8±0.0	1.4±0.2	1.5±0.4	274±39	351±58	520±63
Cellobiohydrolase (CBH)	Desert	8.84±0.26	10.9±1.1	8.84±0.31	87.3±2.4	113±14	114±6.7
	Scrubland	9.47±0.26	1.34±0.52	14.6±4.0	192.8±5.8	67±13	150±30
	Grassland	28.9±1.0	40.5±3.3	34.4±7.9	304±16	327±18	228±29
	Forest	0.9±0.1	1.6±0.3	0.8±0.2	115±12	91±13	83±15
	Subalpine	0.6±0.0	1.0±0.2	1.0±0.3	60.0±6.6	38.4±6.5	67±23
Leucine-aminopeptidase (LAP)	Desert	2.22±0.06	1.41±0.33	2.39±0.47	216.6±9.3	238±21	154±34
	Scrubland	0.95±0.12	3.39±0.64	2.37±0.22	539±89	315±22	179.0±9.8
	Grassland	1.5±0.0	3.4±0.6	5.5±1.5	84.5±2.4	116±12	156±25
	Forest	0.2±0.0	0.3±0.1	0.2±0.0	670±110	400±130	828±230
	Subalpine	0.2±0.0	0.5±0.1	0.2±0.0	810±130	410±150	765±170
N-acetyl-*β*-D-glucosaminidase (NAG)	Desert	4.86±0.10	4.99±0.43	7.8±1.8	62.3±2.2	58.6±4.2	109±31
	Scrubland	6.46±0.15	19.0±1.4	9.9±1.0	100.3±3.7	526±75	159±14
	Grassland	15.9±0.5	13.6±1.6	17.5±2.9	164.5±8.6	140.2±8.4	210±14
	Forest	2.2±0.1	3.3±0.3	3.3±0.3	103.2±7.8	71.6±5.3	117.0±8.1
	Subalpine	0.9±0.0	1.7±0.2	1.8±0.4	76.7±5.3	101±16	105.1±8.6

Table S3 Mean (± SE) Q_{10} of V_{max} for each EE class by site and season. n = number of samples.

		Desert		Scrubland		Grassland		Pine-Oak		Subalpine	
Enzyme	Season	Q_{10}	n	Q_{10}	n	Q_{10}	n	Q_{10}	n	Q_{10}	n
AG	Dry	2.35±0.16	6	2.88±0.37	4	2.10±0.06	6	2.82±0.19	5	1.78±0.17	6
	Wet	2.28±0.06	6	2.51±0.27	6	2.07±0.04	6	3.94±0.94	6	2.71±0.45	6
AP	Dry	1.58±0.03	6	1.60±0.03	6	1.64±0.02	6	1.77±0.04	5	1.53±0.06	6
	Wet	1.64±0.02	6	1.58±0.02	6	1.73±0.03	6	1.94±0.04	6	1.89±0.03	6
BG	Dry	2.04±0.02	6	2.42±0.12	6	1.80±0.03	6	2.26±0.04	5	1.99±0.06	6
	Wet	2.05±0.02	6	1.95±0.05	6	1.89±0.04	6	2.38±0.07	6	2.33±0.07	6
BX	Dry	2.20±0.03	6	2.42±0.10	6	1.99±0.03	6	2.84±0.16	5	2.16±0.16	6
	Wet	2.22±0.02	6	1.99±0.05	6	2.10±0.03	6	3.25±0.23	6	3.25±0.37	6
CBH	Dry	2.55±0.06	6	3.93±0.32	6	2.04±0.02	6	3.21±0.07	5	2.69±0.12	6
	Wet	2.51±0.03	6	2.36±0.06	6	2.06±0.09	6	3.98±0.28	6	3.29±0.30	6
LAP	Dry	2.19±0.06	6	2.29±0.09	6	1.99±0.03	6	2.08±0.08	5	1.78±0.13	4
	Wet	2.09±0.08	6	2.27±0.08	6	1.98±0.12	6	2.28±0.63	4	2.32±0.72	3
NAG	Dry	2.09±0.02	6	1.74±0.02	6	1.90±0.05	6	2.13±0.02	5	2.19±0.08	6
	Wet	2.06±0.08	6	1.90±0.03	6	2.06±0.13	6	2.22±0.03	6	2.63±0.13	6

Table S4 Mean (± SE) Q_{10} of K_m for each EE class by site, across seasons. n = number of samples.

	Desert		Scrubland		Grassland		Pine-Oak		Subalpine	
Enzyme	Q_{10}	n	Q_{10}	n	Q_{10}	N	Q_{10}	n	Q_{10}	n
AG	1.06±0.21	3	1.49±0.15	4	1.22±0.02	9	1.77±0.49	2	0.66±0.02	2
AP	1.22±0.02	8	1.30±0.03	10	1.28±0.07	11	1.28±0.03	11	1.28±0.05	4
BG	1.80±0.04	12	1.67±0.08	9	1.89±0.06	12	1.32±0.02	9	1.37±0.03	11
BX	1.36±0.03	10	1.29±0.03	8	1.39±0.07	11	2.04±0.22	6	2.07±0.24	7
CBH	1.80±0.07	12	2.11±0.11	8	2.06±0.05	11	1.89±0.18	9	1.98±0.34	6
LAP	1.34±0.27	2	1.29±0.06	3	1.20±0.06	8	0.40±0.02	2	0.52±0.08	7
NAG	1.65±0.02	11	1.40±0.03	11	1.52±0.04	12	1.60±0.04	11	1.43±0.06	10

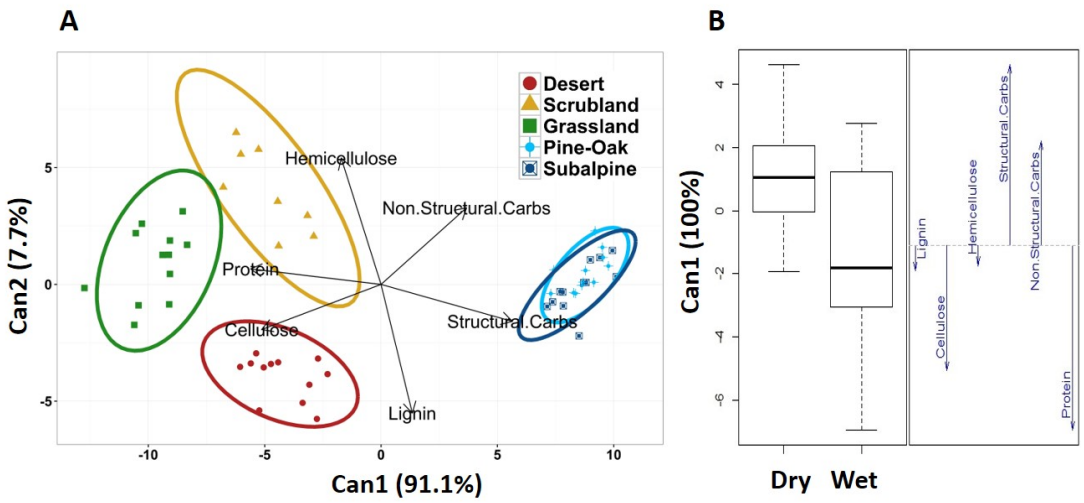

Figure S1. Canonical discriminant analysis for variation in litter chemistry fractions **A)** between sites and **B)** between the dry season (June 2015) and the wet season (December 2015). Loading coefficients – A) Lignin (0.22, -0.91), cellulose (-0.86, -0.32), hemicellulose (-0.29, 0.90), structural carbohydrates (0.94, -0.26), non-structural carbohydrates (0.61, 0.55), protein (-0.93, 0.11). B) Lignin (-0.11), cellulose (-0.54), hemicellulose (-0.09), structural carbohydrates (0.78), non-structural carbohydrates (0.45), protein (-0.79).

6

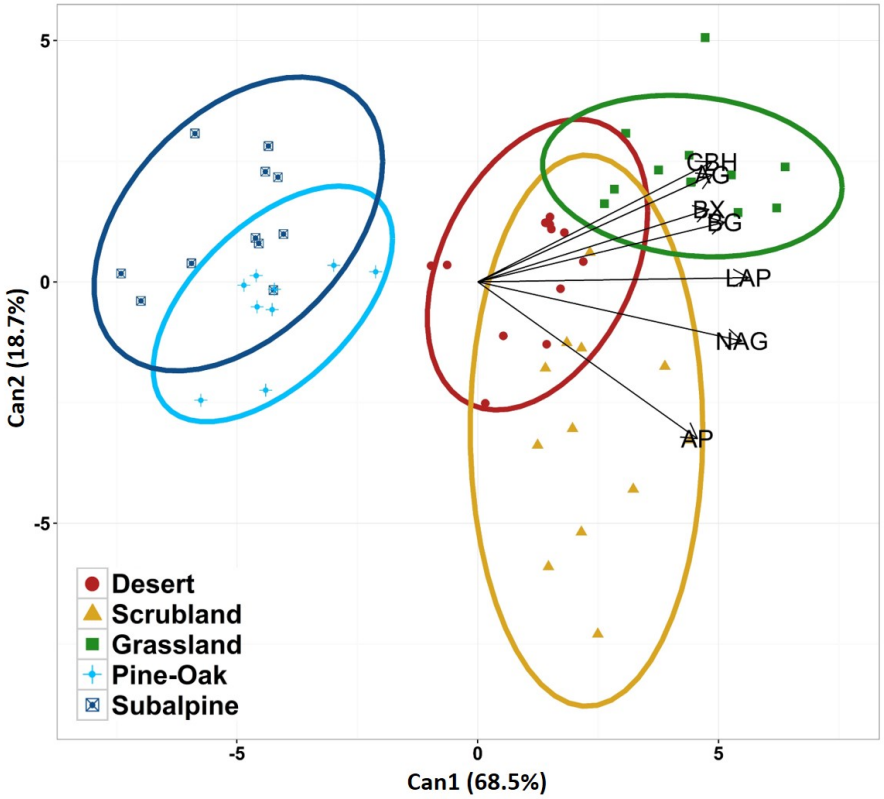

Figure S2. Canonical discriminant analysis for variation in extracellular enzyme V_{max} of all enzyme classes between sites. Loading coefficients – AG (0.81, 0.37), AP (0.76, -0.54), BG (0.85, 0.21), BX (0.80, 0.25), CBH (0.81, 0.41), LAP (0.94, 0.01), NAG (0.91, -0.20).

7

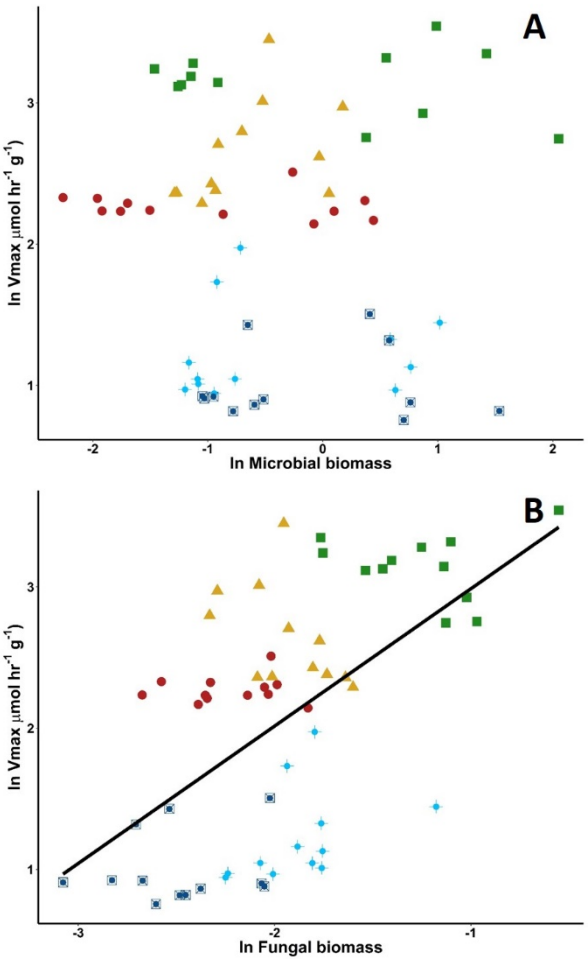

Figure S3. Mean EE V_{max} (μmol hr^{-1} g^{-1}) across the gradient in both seasons a function of **A)** microbial biomass (mg C g^{-1} dry litter, NS) and **B)** fungal biomass (mg C g^{-1} dry litter, $p<0.001$, $R^2=0.30$). October 2014 and December 2015 samples are depicted due to lack of bacterial cell density data for June 2015 samples.

8

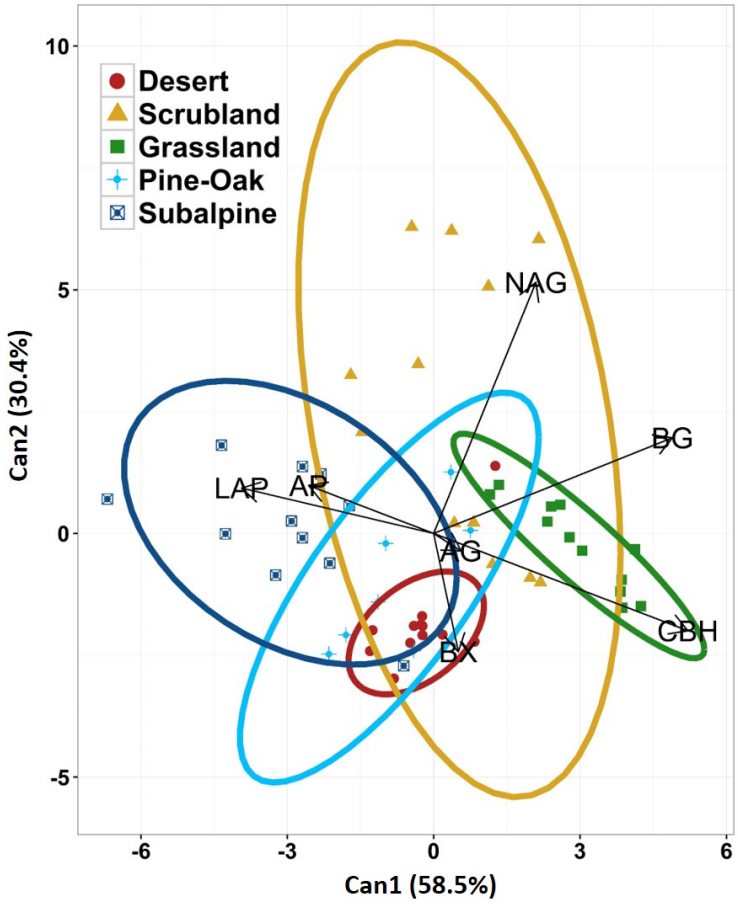

Figure S4. Canonical discriminant analysis for variation in extracellular enzyme K_m of all enzyme classes between sites. Loading coefficients – AG (0.09, -0.06), AP (-0.43, 0.16), BG (0.82, 0.33), BX (0.08, -0.40), CBH (0.87, -0.33), LAP (-0.66, 0.16), NAG (0.35, 0.86).

9

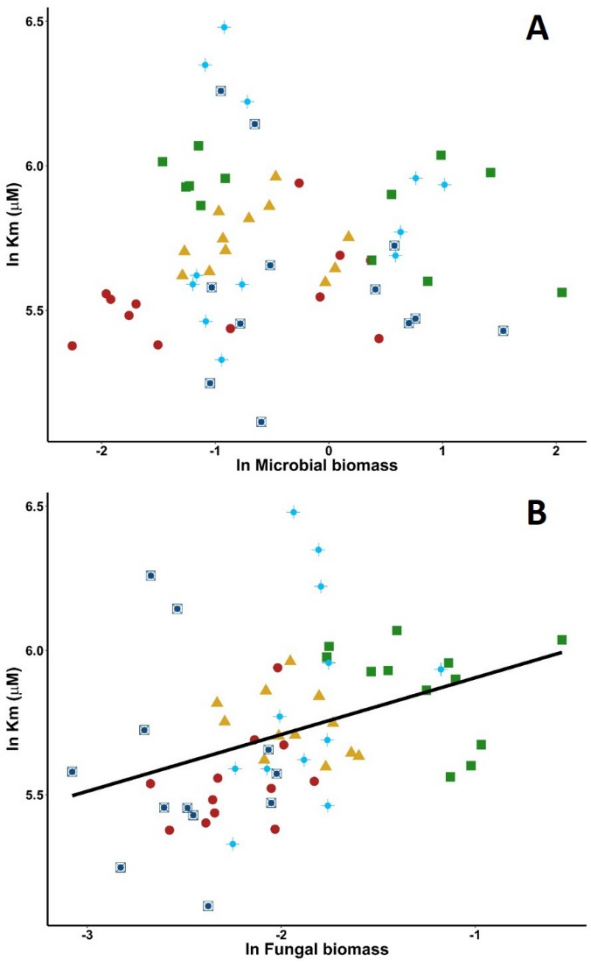

Figure S5. Mean EE K_m (μM) as a function of **A)** microbial biomass (mg C g^{-1} dry litter, NS) and **B)** fungal biomass (mg C g^{-1} dry litter, $p=0.004$, $R^2=0.12$). October 2014 and December 2015 samples are depicted due to lack of bacterial cell density data for June 2015 samples.

10